



Published in final edited form as:

Nat Mater. 2016 February ; 15(2): 190–196. doi:10.1038/nmat4463.

Tough Bonding of Hydrogels to Diverse Nonporous Surfaces

Hyunwoo Yuk¹, Teng Zhang¹, Shaoting Lin¹, German Alberto Parada^{1,2}, and Xuanhe Zhao^{1,3,*}

¹ Soft Active Materials Laboratory, Department of Mechanical Engineering, Massachusetts Institute of Technology, Cambridge, MA 02139, USA

² Department of Chemical Engineering, Massachusetts Institute of Technology, Cambridge, MA 02139

³ Department of Civil and Environmental Engineering, Massachusetts Institute of Technology, Cambridge, MA 02139, USA

In many animals, the bonding of tendon and cartilage to bone is extremely tough (e.g., interfacial toughness $\sim 800 \text{ Jm}^{-2}$)^{1,2}, yet such tough interfaces have not been achieved between synthetic hydrogels and nonporous surfaces of engineered solids³⁻⁹. Here, we report a strategy to design transparent and conductive bonding of synthetic hydrogels containing 90% water to nonporous surfaces of diverse solids including glass, silicon, ceramics, titanium and aluminum. The design strategy is to anchor the long-chain polymer networks of tough hydrogels covalently to nonporous solid surfaces, which can be achieved by the silanation of such surfaces. Compared with physical interactions, the chemical anchorage results in a higher intrinsic work of adhesion and in significant energy dissipation of bulk hydrogel during detachment, which lead to interfacial toughness over 1000 Jm^{-2} . We also demonstrate applications of robust hydrogel-solid hybrids, including hydrogel superglues, mechanically protective hydrogel coatings, hydrogel joints for robotic structures and robust hydrogel-metal conductors.

Hybrid combinations of hydrogels and solid materials including metals, ceramics, glass, silicon and polymers are used in areas as diverse as biomedicine^{10,11}, adaptive and responsive materials¹², antifouling¹³, actuators for optics¹⁴ and fluidics¹⁵, and soft electronics¹⁶ and machines¹⁷. Although hydrogels with extraordinary physical properties have been recently developed³⁻⁹, the weak and brittle bonding between hydrogels and solid

Users may view, print, copy, and download text and data-mine the content in such documents, for the purposes of academic research, subject always to the full Conditions of use:http://www.nature.com/authors/editorial_policies/license.html#terms

* To whom correspondence should be addressed. ; Email: zhaox@mit.edu

Author Contribution

X.Z. and H.Y. conceived the idea. H.Y., T.Z., S.L., G.P. and X.Z. designed the research. H.Y., S.L., and G.P. carried out the experiments and T.Z. performed the numerical simulation. H.Y., T.Z., S.L., G.P. and X.Z. analyzed and interpreted the results. X.Z. drafted the manuscript and all authors contributed to the writing of the manuscript.

Additional information

Supplementary information is available in the online version of the paper. Reprints and permissions information is available online at www.nature.com/reprints. Correspondence and requests for materials should be addressed to X.Z.

Competing financial interests

The authors declare no competing financial interests.

materials often severely hampers their integrations and functions in devices and systems. Whereas intense efforts have been devoted to the development of tough hydrogel-solid interfaces, previous works are generally limited to special cases with porous solid substrates¹⁸. Robust adhesion of dry elastomers to nonporous solids has been achieved^{19,22}, but such adhesion is not applicable to hydrogels that contain significant amounts of water²³. The need for general strategies and practical methods for the design and fabrication of tough hydrogel bonding to diverse solid materials has remained a central challenge for the field.

Here, we report a design strategy and a set of simple fabrication methods to give extremely tough and functional bonding between hydrogels and diverse solids, including glass, silicon, ceramics, titanium and aluminum, to achieve interfacial toughness over 1000 Jm⁻². The new design strategy and fabrication methods do not require porous or topographically patterned surfaces of the solids and allow the hydrogels to contain over 90 wt. % of water. The resultant tough bonding is optically transparent and electrically conductive. In addition, we demonstrate novel functions of hydrogel-solid hybrids uniquely enabled by the tough bonding, including tough hydrogel superglues, hydrogel coatings that are mechanically protective, hydrogel joints for robotic structures and robust hydrogel-metal conductors. The design strategy and simple yet versatile method open new avenues not only to addressing fundamental questions on hydrogel-solid interfaces in biology, physics, chemistry and material science but also to practical applications of robust hydrogel-solid hybrids in diverse areas^{10,17,24}.

The proposed strategy to design tough hydrogel-solid bonding is illustrated in **Fig. 1**. Since interfacial cracks can kink and propagate in relatively brittle hydrogel matrices (see **Video S1**, for example), the design of tough hydrogel-solid bonding first requires high fracture toughness of the constituent hydrogels¹⁸. Whereas tough hydrogels generally consist of covalently-crosslinked long-chain polymer networks that are highly stretchable and other components that dissipate mechanical energy under deformation^{25,26}, it is impractical to chemically bond all components of the hydrogels on solid surfaces. We propose that it is sufficient to achieve relatively tough hydrogel-solid bonding by chemically anchoring the long-chain polymer network of a tough hydrogel on solid surfaces as illustrated in **Fig. 1a**. When such a chemically-anchored tough hydrogel is detached from a solid, the scission of the anchored layer of polymer chains gives the intrinsic work of adhesion Γ_0 ²⁷ (**Fig. 1b**). Meanwhile, the tough hydrogel around the interface will be highly deformed and thus dissipate a significant amount of mechanical energy^{20,22,28}, which further contributes to the interfacial toughness by Γ_D (**Fig. 1b**). Neglecting contributions from mechanical dissipation in the solid and friction on the interface, we can express the total interfacial toughness of the hydrogel-solid bonding as

$$\Gamma = \Gamma_0 + \Gamma_D \quad (1)$$

In Eq. (1), Γ_0 may be much lower than Γ_D for tough hydrogel-solid bonding, but it is still critical to chemically anchor long-chain polymer networks of tough hydrogels on the solids surfaces. This is because the chemical anchorage gives a relatively high intrinsic work of adhesion Γ_0 (compared with physically attached cases), which maintains cohesion of the

hydrogel-solid interface while allowing large deformation and mechanical dissipation to be developed in the bulk hydrogel to give high values of Γ_D (**Fig. 1b**).

To test the proposed design strategy, we use a functional silane, 3-(Trimethoxysilyl) Propyl Methacrylate (TMSPMA), to modify the surfaces of glass, silicon wafer, titanium, aluminum and mica ceramic (**Fig. 2a**)²⁹. We then covalently crosslink the long-chain polymer network of polyacrylamide (PAAm) or polyethylene glycol diacrylate (PEGDA) to the silanes on the modified surfaces of various solids. (See Methods and **Fig. S1a** for details on the modification and anchoring process.) To form tough hydrogels, the long-chain polymer network is interpenetrated with a reversibly-crosslinked network of alginate, chitosan or hyaluronan^{6,26}, in which the reversible crosslinking and chain scission dissipates mechanical energy as illustrated in **Fig. 1a** and **Fig. 1b**. (See Methods for details on the formula and procedures to make various hydrogels.) As control samples, we chemically anchor a pure PAAm or PEGDA hydrogel on silanized solid surfaces, and physically attach the pure PAAm or PEGDA hydrogel and corresponding tough hydrogels on untreated solid surfaces as illustrated in **Fig. 1c**. The shear moduli of all hydrogels in as-prepared states are set to be on the same level, ~ 30 kPa, by controlling the crosslinking densities in the hydrogels.

The samples of tough (e.g., PAAm-alginate) and common (e.g., PAAm) hydrogels chemically anchored and physically attached on glass substrates all look identical, as they are transparent with transmittance over 95%. We demonstrate the transparency of a sample in **Fig. 2b** by placing it above the “MIT MECHÉ” color logo. We then carry out a standard 90-degree peeling test with a peeling rate of 50 mm/min to measure the interfacial toughness between hydrogel sheets with thickness of 3 mm and the glass substrates. A thin (~ 25 μm thick) and rigid glass film backing is attached to the other surface of the hydrogel sheet to prevent its elongation along the peeling direction. Thus, the measured interfacial toughness is equal to the steady-state peeling force per width of the hydrogel sheet³⁰. (See Methods and **Fig. S2** for details of the peeling test.) **Video S1** and **Figs. 2c-e** demonstrate the peeling process of the common hydrogel chemically anchored on the glass substrate. It can be seen that a crack initiates at the hydrogel-solid interface, kinks into the brittle hydrogel, and then propagates forward. The measured interfacial toughness is 24 Jm^{-2} (**Figs. 2i**), limited by the hydrogel's fracture toughness, validating that tough hydrogels are indeed critical in the design of tough hydrogel-solid interfaces. **Video S2** and **Figs. S3** demonstrate a typical peeling process of a tough or common hydrogel physically attached on the glass substrate. Different from the previous process shown in **Video S1** and **Figs. 2c-e**, the crack can easily propagate along the interface without kinking or significantly deforming the hydrogel, giving very low interfacial toughness of 8 Jm^{-2} (**Figs. 2i**). **Video S3** and **Figs. 2f-h** demonstrate the peeling process of the tough hydrogel with its long-chain network chemically anchored on the glass substrate. As the peeling force increases, the hydrogel around the interfacial crack front highly deforms and subsequently becomes unstable^{31,32}, developing a pattern of fingers before the interfacial crack can propagate. When the peeling force reaches a critical value, the crack begins to propagate along the hydrogel-solid interface (**Fig. 2g**). During crack propagation, the fingers coarsen with increasing amplitude and wavelength, and then detach from the substrate (**Fig. 2h**). The measured interfacial toughness is over 1500 Jm^{-2} (**Figs. 2i**), superior to natural counterparts such as tendons and

cartilages on bones. As control cases, we vary the thickness of the tough hydrogel sheet from 1.5mm to 6mm, and obtain similar values of interfacial toughness (**Fig. S4**). We further vary the peeling rate of the test from 200 mm/min to 5 mm/min, and find that the measured interfacial toughness decreases from 3100 Jm^{-2} to 1500 Jm^{-2} accordingly (**Fig. S5**). It is evident that the measured interfacial toughness of chemically anchored PAAm-alginate hydrogel is rate-dependent, possibly due to viscoelasticity of the hydrogel (**Fig. S5**). Furthermore, the peeling rate used in the current study (50 mm/min) gives an interfacial toughness around the lower asymptote, which reflects the effects of intrinsic work of adhesion and rate-independent dissipation such as Mullins effect³³.

To understand the phenomena described above and the interfacial toughening mechanism, we develop a finite-element model to simulate the peeling process of a hydrogel sheet from rigid substrate under plane-strain condition. In the model, the intrinsic work of adhesion Γ_0 is characterized by a layer of cohesive elements and the dissipative property of the PAAm-alginate hydrogel is characterized by Mullins effect³³. (See Supplementary Information and **Fig. S13-19** and **Video S8, S9** for details of the model.) **Figure 2j** gives the calculated relation between the intrinsic work of adhesion Γ_0 and the interfacial toughness Γ . It is evident that the interfacial toughness increases monotonically with the intrinsic work of adhesion, which is effectively augmented by a factor determined by the dissipative properties of the hydrogel. We also vary the thickness of the PAAm-alginate hydrogel in the model from 0.8 mm to 6 mm and find that the calculated interfacial toughness is approximately the same, consistent with the experimental observation (**Fig. S4** and **Fig. S19**). As a control case, we model the peeling test of a hydrogel with no Mullins effect (i.e., no dissipation) but otherwise the same mechanical properties as the PAAm-alginate hydrogel. From **Fig. 2j**, it is evident that the calculated interfacial toughness for the control case is approximately the same as the prescribed the intrinsic work of adhesion. Although the current finite-element model does not account for the effects of fingering instability or viscoelasticity on mechanical dissipation, it clearly demonstrates that high values of the intrinsic work of adhesion and significant mechanical dissipation of the bulk hydrogel are key to design tough bonding of hydrogels on solids (**Fig. 2j**).

The proposed design strategy and fabrication methods for tough hydrogel-solid bonding is applicable to multiple types of nonporous solid materials. **Figure 3a** shows that the measured interfacial toughness is consistently high for the PAAm-alginate tough hydrogel chemically anchored on glass (1500 Jm^{-2}), silicon (1500 Jm^{-2}), aluminum (1200 Jm^{-2}), titanium (1250 Jm^{-2}) and ceramics (1300 Jm^{-2}). Replacing the PAAm-alginate with other types of tough hydrogels including PAAm-hyaluronan, PAAm-chitosan, PEGDA-alginate and PEGDA-hyaluronan still yields relatively high interfacial toughness, $148 - 820 \text{ Jm}^{-2}$, compared with the interfacial toughness in controlled cases, $4.4 - 16 \text{ Jm}^{-2}$ (**Fig. S6**). (See Methods for details on other hydrogel-solid bonding). To explain the difference in interfacial toughness of different tough hydrogels with long-chain networks chemically anchored on substrates, we measure the maximum dissipative capacity and fracture toughness of these hydrogels (**Fig. S7**). It can be seen that, for tough hydrogels with the same chemically-anchored long-chain networks (i.e., PAAm-based or PEGDA-based tough hydrogels), both the interfacial toughness and fracture toughness increase with the maximum dissipative

capacity of the hydrogels (**Fig. S7**). These results validate that significant energy dissipation in bulk hydrogels is critical to achieving high interfacial toughness.

Since hydrogels are commonly used in wet environments, we further immerse the PAAm-alginate hydrogels with PAAm networks anchored on various solid substrates in water for 24 hours to allow the hydrogels to swell to equilibrium states. We find that the anchored hydrogels do not detach from the solid substrates in swollen state. The interfacial toughness of the swollen samples is measured using the 90-degree-peeling test. From **Video S4**, it can be seen that the detaching process of the swollen hydrogel is similar to that of the same hydrogel in as-prepared state (i.e., **Fig. 2f-h** and **Video S3**). As shown in **Fig. S8b** and **Fig. 3a**, the measured interfacial toughness for swollen hydrogels bonded on glass (1123 Jm^{-2}), silicon (1210 Jm^{-2}), aluminum (1046 Jm^{-2}), titanium (1113 Jm^{-2}) and ceramics (1091 Jm^{-2}) are consistently high, indicating that the design strategy and fabrication methods can give tough bonding of hydrogels to diverse solids in wet environment. The slight decrease in interfacial toughness from as-prepared to swollen hydrogels may be due to the decrease of dissipative capability of hydrogels³⁴ and/or the residual stress generated in the hydrogels during swelling.

The above results prove that chemically anchoring the long-chain networks of tough hydrogels on solid substrates can lead to tough hydrogel-solid bonding. Since the tough hydrogels used in the current study are composed of covalently-crosslinked long-chain networks and reversibly-crosslinked dissipative networks, it is also important to know the effects of chemically anchoring dissipative networks on the resultant interfacial toughness. We chemically anchor the dissipative networks (i.e., alginate or hyaluronan) in PAAm-alginate, PEGDA-alginate and PEGDA-hyaluronan hydrogels on glass substrates using EDC-Sulfo NHS chemistry, and then measure the interfacial toughness of resultant samples (see **Fig. S1b-c** and Methods for details on anchoring alginate and hyaluronan). As shown in **Fig. S9a-b**, the measured interfacial toughness for PEGDA-alginate and PEGDA-hyaluronan hydrogels with dissipative network anchored on substrates is 13 Jm^{-2} and 16 Jm^{-2} respectively – much lower than the values of the same hydrogels with long-chain networks anchored on substrates (365 Jm^{-2} and 148 Jm^{-2} respectively). On the other hand, the interfacial toughness for PAAm-alginate hydrogel with alginate anchored on substrate is 1450 Jm^{-2} (**Fig. S9c**), similar to the value of PAAm-alginate hydrogel with PAAm anchored on substrate (1500 Jm^{-2}). It is evident that anchoring either long-chain or dissipative networks gives similar interfacial toughness in PAAm-alginate hydrogel but very different values in PEGDA-alginate (or PEGDA-hyaluronan) hydrogel (**Fig. S9**). The different results obtained in PAAm-alginate and PEGDA-alginate (or PEGDA-hyaluronan) hydrogels may be due to much stronger interactions between long-chain and dissipative networks in PAAm-alginate hydrogel than in PEGDA-alginate and PEGDA-hyaluronan hydrogels.^{6,35}

To compare our results with existing works in the field, we summarize the interfacial toughness of various hydrogel-solid bonding commonly used in engineering applications vs. water concentrations in those hydrogels in **Fig. 3b**. (See supplementary materials and **Fig. S10** for detailed references). Whereas our approach allows the PAAm-alginate tough hydrogels to contain 90 wt. % of water and does not require porous or topographically patterned surfaces of the solids, it can achieve extremely high interfacial toughness up to

1500 Jm⁻². In comparison, most of synthetic hydrogel bonding has relatively low interfacial toughness, below 100 Jm⁻². Although previous work on hydrogels and animal skin tissues impregnated in porous substrates gave interfacial toughness up to 1000 Jm⁻², the hydrogels and tissues contains 60 to 80 wt. % water and the requirement of porous solids significantly limits their applications¹⁸. Further notably, our fabrication methods of tough hydrogel bonding are relatively simple compared with previous methods and generally applicable to a wide range of hydrogels and solid materials.

Owing to its simplicity and versatility, the design strategy and fabrication methods for tough hydrogel-solid bonding can potentially enable a set of unprecedented functions of hydrogel-solid hybrids. For example, the tough hydrogels may be used as soft (e.g., 30 kPa), wet (e.g., with 90% water) and biocompatible³⁶ superglues for glass, ceramics and Ti, which have been used in biomedical applications. (See Methods and **Fig. S12** for details on biocompatibility of tough hydrogels bonded on solid surfaces.) **Figure 4a** demonstrates that two glass plates bonded by the tough hydrogel superglue (dimension, 5 cm × 5 cm × 1.5 mm) are transparent, and can readily sustain a weight of 25 kg. (See Methods for details on fabrication of hydrogel superglue.) As another example, the tough hydrogel-solid bonding can re-define the functions and capabilities of commonly-used hydrogel coatings, which are usually mechanically fragile and susceptible to debonding failure. **Video S5 and Fig. 4b** demonstrates the process of shattering and consequently deforming a silicon wafer coated with a layer of chemically-anchored tough hydrogel. Thanks to the high toughness of the hydrogel and interface, the new coating prevents detachment of the shattered pieces of silicon wafer and maintains integrity of the hydrogel-solid hybrid even under high stretch of 3 times, demonstrating hydrogel coating's new capability of mechanical protection and support. (See Methods for details on fabrication of mechanically protective hydrogel coating.) The tough hydrogel bonding can also be used as compliant joints in mechanical and robotic structures. **Video S6 and Fig. 4c** demonstrate an example of four ceramic bars bonded with the chemically-anchored tough hydrogels. The compliance of the hydrogel combined with high toughness of the bonding enables versatile modes of deformation of the structure. (See Methods for details on fabrication of hydrogel joints.) In addition, the tough hydrogel bonding is electrically conductive and thus can provide a robust interface between hydrogel ionic conductors and metal electrodes¹⁶. Existing hydrogel-metal interfaces usually rely on conductive copper tapes whose robustness is uncertain. **Video S7 and Fig. 4d** demonstrate that the hybrid combination of a tough hydrogel chemically anchored on two titanium electrodes is conductive enough to power a LED light, even when the hydrogel is under high stretch of 4.5 times. In addition, the conductivity of the hydrogel-metal hybrid maintains almost the same even after 1000 cycles of high stretch up to 4 times. (See Methods and **Fig. S11** for details on fabrication of robust hydrogel-metal conductors and measurement on its electrical conductivity.)

In summary, we demonstrate that the chemical anchorage of long-chain polymer networks of tough hydrogels on solid surfaces represents a general strategy to design tough and functional bonding between hydrogels and diverse solids. Following the design strategy, we use simple methods such as silane modification and EDC chemistry to achieve tough, transparent and conductive bonding of hydrogels to glass, ceramic, silicon wafer, aluminum

and titanium with interfacial toughness over 1000 Jm^{-2} — superior to the toughness of tendon-bone and cartilage-bone interfaces. The ability to fabricate extremely robust hydrogel-solid hybrids makes a number of future research directions and applications possible. For example, electronic devices robustly embedded in (or attached on) tough hydrogels may lead to a new class of stretchable hydrogel electronics, which are softer, wetter and more biocompatible than existing ones based on dry elastomers matrices. New microfluidic systems based on tough hydrogels bonded on nonporous substrates may be able to sustain high flow rate, high pressure and large deformation to better approximate physiological environments than existing microfluidics based on weak or brittle hydrogels. Neural probes coated with tough and bio-compatible hydrogels with reduced rigidity³⁴ may be used to better match the mechanical and physiological properties of brains, spinal cords and peripheral nervous systems.

Methods

Materials

Unless otherwise specified, the chemicals used in the current work were purchased from Sigma-Aldrich and used without further purification. For the long-chain polymer networks in the hydrogels, acrylamide (AAM; Sigma-Aldrich A8887) was the monomer used for the polyacrylamide (PAAm) networks, and 20 kDa polyethylene glycol diacrylate (PEGDA) was the macromonomer used for the PEGDA networks. The PEGDA macromonomers were synthesized based on a previously reported protocol³⁷ using polyethylene glycol (PEG; Sigma-Aldrich 81300), acryloyl chloride (Sigma-Aldrich 549797), triethylamine (TEA; Sigma-Aldrich 471283), dichloromethane (Sigma-Aldrich 270997), sodium bicarbonate (Sigma-Aldrich S6014), magnesium sulfate (Sigma-Aldrich M7506) and diethyl ether (Sigma-Aldrich 346136). For the polyacrylamide (PAAm) hydrogel, N,N-methylenebisacrylamide (MBAA; Sigma-Aldrich 146072) was used as crosslinker, ammonium persulfate (APS; Sigma-Aldrich A3678) as thermal initiator and N,N,N',N'-tetramethylethylenediamine (TEMED; Sigma-Aldrich T9281) as crosslinking accelerator. For the PEGDA hydrogel, 2-Hydroxy-4'-(2-hydroxyethoxy)-2-methylpropiophenone (Irgacure 2959; Sigma-Aldrich 410896) was used as photo initiator. For the dissipative polymer networks in tough hydrogels, a number of ionically crosslinkable biopolymers were used including sodium alginate (Sigma-Aldrich A2033) ionically crosslinked with calcium sulfate (Sigma-Alginate C3771), chitosan (Sigma-Aldrich 740500) ionically crosslinked with sodium tripolyphosphate (TPP; Sigma-Aldrich 238503), and sodium hyaluronan (HA; Sigma-Aldrich H5542) ionically crosslinked with iron chloride (Sigma-Aldrich 157740). For chemical modification of various solid materials, functional silane 3-(Trimethoxysilyl) propyl methacrylate (TMSPMA; Sigma-Aldrich 440159) and acetic acid (Sigma-Aldrich 27225) were used. For anchoring alginate and hyaluronan on solid substrates, (3-Aminopropyl) Triethoxysilane (APTES, Sigma-Aldrich 440140), N-Hydroxysulfosuccinimide (Sulfo-NHS, Sigma-Aldrich 56485), N-(3-Dimethylaminopropyl)-N' ethylcarbodiimide (EDC, Sigma-Aldrich 39391), 2-(N-Morpholino)ethanesulfonic acid (MES, Sigma-Aldrich M3671) and Sodium Chloride (Sigma-Aldrich 746398) were used.

In the 90-degree peeling experiments, borosilicate glass (McMaster Carr), silicon wafers with a thermal oxidized layer (UniversityWafer), nonporous glass mica ceramic (McMaster Carr), anodized aluminum (Inventables) and titanium (McMaster Carr) plates were used as the solid substrates. As a stiff backing for the hydrogel sheet, ultrathin glass films (25 μm ; Schott Advanced Optics) were used together with transparent Scotch tape (3M). In the conductive hydrogel-metal bonding experiments, sodium chloride solution was used as an electrolyte.

Synthesis of various tough hydrogels

The PAAm-alginate tough hydrogel was synthesized by mixing 10 mL of a carefully degassed aqueous precursor solution (12.05 wt. % AAm, 1.95 wt. % sodium alginate, 0.017 wt. % MBAA and 0.043 wt. % APS) with calcium sulfate slurry (0.1328 times the weight of sodium alginate) and TEMED (0.0025 times the weight of AAm)⁶. The mixture was mixed quickly and poured into a laser-cut Plexiglass acrylic mold. The lid of the mold included an opening for the functionalized substrates to be in contact with hydrogel precursor solution. The gel was crosslinked by UV light irradiation for an hour (254 nm UV with 6.0 mWcm^{-2} average intensity; Spectrolinker XL-1500).

The PAAm-hyaluronan tough hydrogel was synthesized by mixing 10 mL of degassed precursor solution (18 wt. % AAm, 2 wt. % HA, 0.026 wt. % MBAA and 0.06 wt. % APS) with 60 μL of iron chloride solution (0.05 M) and TEMED (0.0025 times the weight of AAm). The PAAm-chitosan tough hydrogel was synthesized by mixing 10 mL of degassed precursor solution (24 wt. % AAm, 2 wt. % chitosan, 0.034 wt. % MBAA and 0.084 wt. % APS) with 60 μL of TPP solution (0.05 M) and TEMED (0.0025 times the weight of AAm). The PEGDA-alginate tough hydrogel was synthesized by mixing 10 mL of a degassed precursor solution (20 wt. % PEGDA and 2.5 wt. % sodium alginate) with calcium sulfate slurry (0.068 times the weight of sodium alginate) and Irgacure 2959 (0.0018 the weight of PEGDA). The PEGDA-hyaluronan tough hydrogel was synthesized by mixing 10 mL of a degassed precursor solution (20 wt. % PEGDA and 2 wt. % HA) with 60 μL of iron chloride solution (0.05 M) and Irgacure 2959 (0.0018 the weight of PEGDA). The curing procedure was identical to the PAAm-alginate tough hydrogel.

Common PAAm hydrogel was synthesized by mixing 10 mL of degassed precursor solution (23 wt. % AAm, 0.051 wt. % MBAA and 0.043 wt. % APS) and TEMED (0.0025 times the weight of AAm). The curing procedure was identical to the PAAm-alginate tough hydrogel. Note that the modulus of the common PAAm hydrogel was tuned to match the PAAm-alginate tough hydrogel's modulus (30 kPa) based on the previously reported data⁶.

Chemically anchoring PAAm and PEGDA on various solid surfaces

The surface of various solids was functionalized by grafting functional silane TMSPMA. Solid substrates were thoroughly cleaned with acetone, ethanol and deionized water in that order, and completely dried before the next step. Cleaned substrates were treated by oxygen plasma (30 W with 200 mTorr pressure; Harrick Plasma PDC-001) for 5 min. Right after the plasma treatment, the substrate surface was covered with 5 mL of the silane solution (100 mL deionized water, 10 μL of acetic acid with pH 3.5 and 2 wt. % of TMSPMA) and

incubated for 2 hours at room temperature. Substrates were washed with ethanol and completely dried. Functionalized substrates were stored in low humidity conditions before being used for experiments.

During oxygen plasma treatment of the solids, oxide layers on the surfaces of the solids (silicon oxide on glass and silicon wafer, aluminum oxide on aluminum, titanium oxide on titanium, and metal oxides on ceramics) react to hydrophilic hydroxyl groups by oxygen radicals produced by oxygen plasma. These hydroxyl groups on the oxide layer readily form hydrogen bonds with silanes in the functionalization solution generating a self-assembled layer of silanes on the oxide layers³⁸. Notably, the methoxy groups in TMSPMA are readily hydroxylated in acidic aqueous environment and formed silanes. These hydrogen bonds between surface oxides and silanes become chemically stable siloxane bonds with removal of water, forming strongly grafted TMSPMA onto oxide layers on various solids³⁹.

Grafted TMSPMA has a methacrylate terminal group which can copolymerize with the acrylate groups in either AAm or PEGDA under free radical polymerization process, generating chemically anchored long-chain polymer network onto various solid surfaces⁴⁰. Since the long-chain polymer networks in hydrogels are chemically anchored onto solid surfaces via strong and stable covalent bonds, the interfaces can achieve higher intrinsic work of adhesion than physically attached hydrogels. The silane functionalization chemistry is summarized in **Fig. S1a**.

Chemically anchoring alginate and hyaluronan on various solid surfaces

We anchored alginate and hyaluronan via EDC-Sulfo NHS chemistry following previously reported protocols^{41,42} (**Fig. S1b-c**). Glass substrates were cleaned and oxygen plasma treated following the abovementioned procedures and covered with 5 mL of the amino-silane solution (100 mL deionized water, 2 wt. % of APTES) and incubated for 2 hours at room temperature. Substrates were washed with ethanol and completely dried. The amino-silane functionalized glass substrates were further incubated in either alginate anchoring solution or hyaluronan anchoring solution (100 mL of aqueous MES buffer (0.1 M MES and 50 mM sodium chloride), 1 wt. % alginate or hyaluronan, Sulfo-NHS (molar ratio of 30:1 to either alginate or hyaluronan) and EDC (molar ratio of 25:1 to either alginate or hyaluronan)) for 24 hours. Incubated glass substrates were finally washed with deionized water and completely dried before use.

Interfacial toughness measurement

All tests were conducted in ambient air at room temperature. The hydrogels and hydrogel-solid interfaces maintain consistent properties over the time of the tests (i.e., ~ a few minutes), during which the effect of dehydration is not significant. Whereas long-term dehydration will significantly vary the properties of hydrogels, adding highly hydratable salts into the hydrogels can enhance their water retention capacity⁴³. The interfacial toughness of various hydrogel-solid bonding was measured using the standard 90-degree peeling test (ASTM D 2861) with mechanical testing machine (2 kN load cell; Zwick / Roell Z2.5) and 90-degree peeling fixture (TestResources, G50). All rigid substrates were prepared with 7.62 cm in width, 12.7 cm in length and 0.32 cm in thickness. Hydrogels were cured on

the solid substrates within Plexiglass acrylic mold with size of 110 mm × 30 mm × 6 mm. As a stiff backing for the hydrogel, TMSPMA grafted ultrathin glass film was used with an additional protective layer of transparent Scotch tape (3M) on top of the glass film. Prepared samples were tested with the standard 90-degree peeling test setup (**Fig. S2**). All 90-degree peeling tests were performed with constant peeling speed of 50 mm/min. The measured force reached a plateau as the peeling process entered steady state, and this plateau force was calculated by averaging the measured force values in the steady state region with common data processing software (**Fig. S8a**). The interfacial toughness T was determined by dividing the plateau force F by the width of the hydrogel sheet W . To test the dependence of interfacial toughness on hydrogel thickness, we carried out a set of 90-degree peeling tests on PAAm-alginate hydrogels with different thicknesses (1.5 mm ~ 6 mm) chemically anchored on glass substrates (**Fig. S4a**). For interfacial toughness measurement of fully swollen samples, each peeling test samples was immersed in deionized water for 24 hours and tested by the standard 90-degree peeling test (**Fig. S8b**).

To demonstrate the peeling rate dependency of the measured interfacial toughness, we performed a set of 90-degree peeling tests on PAAm-alginate hydrogels chemically anchored on glass substrates with varying peeling rates from 5 mm/min (lowest) to 200 mm/min (highest) (**Fig. S5**).

To demonstrate that the proposed strategy and method is generally applicable to multiple types of hydrogels, we also performed standard 90-degree peeling tests on various types of tough hydrogels including PAAm-hyaluronan, PAAm-chitosan, PEGDA-alginate and PEGDA-hyaluronan hydrogels chemically anchored on glass substrates (**Fig. S6a**). The measured interfacial toughness for these tough hydrogels (148 – 820 Jm⁻², **Fig. S6b**) was consistently much higher than the interfacial toughness of the control cases (4.4 – 16 Jm⁻², **Fig. S6b**).

Preparation of hydrogel superglue, coating and joints

For the hydrogel superglue, two TMSPMA grafted glass plates (5 cm × 12 cm × 2 cm) were connected by thin tough hydrogel (5 cm × 5 cm × 1.5 mm) and subjected to weight up to 25 kg. Weight was applied by hanging metal pieces of known weights with metal wires. Hydrogel joints were fabricated by curing tough hydrogel using Plexiglass acrylic mold between four TMSPMA grafted nonporous glass mica ceramic rods (75 mm length with 10 mm diameter) forming an interconnected square structure. To test the robustness of these hydrogel joints, each joint was twisted and rotated to large angles. Hydrogel coating was fabricated by curing a thin (1 mm) tough hydrogel layer onto the TMSPMA grafted thermal oxide silicon wafer (100 μm thickness with 50.8 mm diameter). To test the hydrogel coating's protective capability, we shattered the wafer with metal hammer and stretched the hydrogel-coated wafer by hand up to 3 times of its original diameter. In preparation of samples, we used the PAAm-alginate tough hydrogel. The grafting of TMSPMA on various solids was conducted as discussed in the previous section.

Electrically conductive hydrogel interface

Ionic tough hydrogel was prepared by curing tough PAAm-alginate hydrogel on two TMSPMA grafted titanium slabs and then soaking in sodium chloride solution (3 M) for 6 hours. The electric resistance of the ionic hydrogel-titanium hybrid was measured using the four-point method⁴⁴. The ionic hydrogel-titanium hybrid was connected in series with a function generator and galvanometer, and the voltage between titanium slabs was measured with a voltmeter connected in parallel (**Fig. S11a**). The ratio of the measured voltage to the measured current gave the electric resistance of ionic hydrogel-titanium hybrid. The resistivity was then calculated using the relation $R = \rho L/A$ for a given geometry of the ionic hydrogel in test where ρ is resistivity, L length of the gel and A cross-sectional area. The rate of stretch was kept constant at 100 mm/min using a mechanical testing machine. All electric connections other than the ionic tough hydrogel-titanium interface were established using conductive aluminum tapes. Cyclic extension of the ionic tough hydrogel was done by mechanical testing machine based on predetermined numbers of cycles. The ionic tough hydrogel's ability to transmit power was tested by lighting up LEDs using AC power source (1 kHz 5V peak-to-peak sinusoidal). **Figure S11b** illustrates the test setup.

Biocompatibility of tough hydrogel bonding

The biocompatibility of tough hydrogels including PAAm-alginate and PEGDA-alginate hydrogels has been validated in previous studies^{35,36}. In the current study, the biocompatibility of PAAm-alginate hydrogel bonded on silane-grafted glass was tested *in vitro* with a live/dead viability assay of hTERT-immortalized human Mesenchymal Stem Cells (MSCs) (**Fig. S12**). A hydrogel disk was chemically anchored on a glass slide following the abovementioned procedure using TMSPMA and then swelled in PBS for two days. To focus on the biocompatibility of the hydrogel-solid interface, the hydrogel was peeled off from the glass slide to expose the previously bonded interface. Thereafter, both the hydrogel and the glass slide were placed in 24-well plates with the exposed interfaces facing up (**Fig. S12a**). MSCs were seeded at a density of 25,000 cells/well on the exposed interfaces of hydrogel and glass, and incubated for seven days at 37 °C and 5% CO₂ in complete cell culture media (high-glucose DMEM with 10% FBS, 1mM sodium pyruvate, 1X MEM (non-essential amino acids), 2mM glutamax, and 100U/mL penicillin-streptomycin) from Life Technologies.

A life/dead staining was performed using the LIVE/DEAD kit for mammalian cells (Life Technologies) per manufacturer's instructions, and fluorescent images were obtained using a Leica DMI 6000 microscope with Oasis Surveyor software. As seen in **Fig. S12c**, the MSCs proliferated and survived on the exposed interface of the glass slide. On the exposed interface of the hydrogel, there was a lower number of cells as the MSCs did not attach well on the hydrogel, but most cells that attached were alive, consistent with previous report³⁶ (**Fig. S12b**). In both cases, the percentage of viable MSCs on the exposed interfaces is over 95 % after seven days of incubation. (It should be noted that although the formed tough hydrogel-glass interface is biocompatible, the bonding process is not since AAm monomers used in the process are toxic.)

Supplementary Material

Refer to Web version on PubMed Central for supplementary material.

Acknowledgement

The authors thank Alex Wang and Prof. Linda Griffith for their help on the cell viability test. This work is supported by ONR (No. N00014-14-1-0528), MIT Institute for Soldier Nanotechnologies and NSF (No. CMMI-1253495). H. Y. acknowledges the financial support from Samsung Scholarship. X. Z. acknowledges the supports from NIH (No. UH3TR000505) and MIT Materials Research Science and Engineering Center.

Reference

1. Bobyn J, Wilson G, MacGregor D, Pilliar R, Weatherly G. Effect of pore size on the peel strength of attachment of fibrous tissue to porous - surfaced implants. *Journal of biomedical materials research*. 1982; 16:571–584. [PubMed: 7130213]
2. Moretti M, et al. Structural characterization and reliable biomechanical assessment of integrative cartilage repair. *Journal of biomechanics*. 2005; 38:1846–1854. [PubMed: 16023472]
3. Gong JP, Katsuyama Y, Kurokawa T, Osada Y. Double-network hydrogels with extremely high mechanical strength. *Advanced Materials*. 2003; 15:1155. doi:10.1002/adma.200304907.
4. Wang Q, et al. High-water-content mouldable hydrogels by mixing clay and a dendritic molecular binder. *Nature*. 2010; 463:339–343. [PubMed: 20090750]
5. Henderson KJ, Zhou TC, Otim KJ, Shull KR. Ionically cross-linked triblock copolymer hydrogels with high strength. *Macromolecules*. 2010; 43:6193–6201.
6. Sun J-Y, et al. Highly stretchable and tough hydrogels. *Nature*. 2012; 489:133–136. doi:10.1038/nature11409. [PubMed: 22955625]
7. Sun TL, et al. Physical hydrogels composed of polyampholytes demonstrate high toughness and viscoelasticity. *Nat Mater*. 2013; 12:932. doi:10.1038/nmat3713. [PubMed: 23892784]
8. Kamata H, Akagi Y, Kayasuga-Kariya Y, Chung U-i, Sakai T. “Nonswellable” Hydrogel Without Mechanical Hysteresis. *Science*. 2014; 343:873–875. [PubMed: 24558157]
9. Liu M, et al. An anisotropic hydrogel with electrostatic repulsion between cofacially aligned nanosheets. *Nature*. 2015; 517:68–72. [PubMed: 25557713]
10. Peppas NA, Hilt JZ, Khademhosseini A, Langer R. Hydrogels in biology and medicine: from molecular principles to bionanotechnology. *Advanced Materials*. 2006; 18:1345–1360.
11. Lee KY, Mooney DJ. Hydrogels for tissue engineering. *Chemical reviews*. 2001; 101:1869–1880. [PubMed: 11710233]
12. Sidorenko A, Krupenkin T, Taylor A, Fratzl P, Aizenberg J. Reversible switching of hydrogel-actuated nanostructures into complex micropatterns. *Science*. 2007; 315:487–490. [PubMed: 17255505]
13. Banerjee I, Pangule RC, Kane RS. Antifouling coatings: recent developments in the design of surfaces that prevent fouling by proteins, bacteria, and marine organisms. *Advanced Materials*. 2011; 23:690–718. [PubMed: 20886559]
14. Dong L, Agarwal AK, Beebe DJ, Jiang H. Adaptive liquid microlenses activated by stimuli-responsive hydrogels. *Nature*. 2006; 442:551–554. [PubMed: 16885981]
15. Beebe DJ, et al. Functional hydrogel structures for autonomous flow control inside microfluidic channels. *Nature*. 2000; 404:588–590. [PubMed: 10766238]
16. Keplinger C, et al. Stretchable, transparent, ionic conductors. *Science*. 2013; 341:984–987. [PubMed: 23990555]
17. Yu C, et al. Electronically Programmable, Reversible Shape Change in Two - and Three - Dimensional Hydrogel Structures. *Advanced Materials*. 2013; 25:1541–1546. [PubMed: 23255239]
18. Kurokawa T, Furukawa H, Wang W, Tanaka Y, Gong JP. Formation of a strong hydrogel–porous solid interface via the double-network principle. *Acta biomaterialia*. 2010; 6:1353–1359. [PubMed: 19887124]

19. Ahagon A, Gent A. Effect of interfacial bonding on the strength of adhesion. *Journal of Polymer Science: Polymer Physics Edition*. 1975; 13:1285–1300.
20. Gent A. Adhesion and strength of viscoelastic solids. Is there a relationship between adhesion and bulk properties? *Langmuir : the ACS journal of surfaces and colloids*. 1996; 12:4492–4496.
21. Kaelble D. Peel adhesion: influence of surface energies and adhesive rheology. *The Journal of Adhesion*. 1969; 1:102–123.
22. Derail C, Allal A, Marin G, Tordjeman P. Relationship between viscoelastic and peeling properties of model adhesives. Part 1. Cohesive fracture. *The Journal of Adhesion*. 1997; 61:123–157.
23. Sudre G, Olanier L, Tran Y, Hourdet D, Creton C. Reversible adhesion between a hydrogel and a polymer brush. *Soft Matter*. 2012; 8:8184–8193.
24. Weissman JM, Sunkara HB, Albert ST, Asher SA. Thermally switchable periodicities and diffraction from mesoscopically ordered materials. *Science*. 1996; 274:959–963. [PubMed: 8875932]
25. Gong JP. Why are double network hydrogels so tough? *Soft Matter*. 2010; 6:2583–2590.
26. Zhao X. Multi-scale multi-mechanism design of tough hydrogels: building dissipation into stretchy networks. *Soft Matter*. 2014; 10:672–687. [PubMed: 24834901]
27. Lake GJ, Thomas AG. STRENGTH OF HIGHLY ELASTIC MATERIALS. *Proceedings of the Royal Society of London Series a-Mathematical and Physical Sciences*. 1967; 300:108. doi: 10.1098/rspa.1967.0160.
28. Webber RE, Creton C, Brown HR, Gong JP. Large strain hysteresis and Mullins effect of tough double-network hydrogels. *Macromolecules*. 2007; 40:2919–2927. doi:10.1021/ma062924y.
29. Tegelström H, Wyöni PI. Silanization of supporting glass plates avoiding fixation of polyacrylamide gels to glass cover plates. *Electrophoresis*. 1986; 7:99–99.
30. Kendall K. Thin-film peeling—the elastic term. *Journal of Physics D: Applied Physics*. 1975; 8:1449.
31. Ghatak A, Chaudhury MK, Shenoy V, Sharma A. Meniscus instability in a thin elastic film. *Physical Review Letters*. 2000; 85:4329. [PubMed: 11060630]
32. Biggins JS, Saintyves B, Wei Z, Bouchaud E, Mahadevan L. Digital instability of a confined elastic meniscus. *Proceedings of the National Academy of Sciences*. 2013; 110:12545–12548.
33. Ogden R, Roxburgh D. A pseudo-elastic model for the Mullins effect in filled rubber. *Proceedings of the Royal Society of London. Series A: Mathematical, Physical and Engineering Sciences*. 1999; 455:2861–2877.
34. Lin S, Zhou Y, Zhao X. Designing extremely resilient and tough hydrogels via delayed dissipation. *Extreme Mechanics Letters*. 2014; 1:70.
35. Hong S, et al. 3D Printing of Highly Stretchable and Tough Hydrogels into Complex, Cellularized Structures. *Advanced Materials*. 2015; 27:4035–4040. [PubMed: 26033288]
36. Darnell MC, et al. Performance and biocompatibility of extremely tough alginate/polyacrylamide hydrogels. *Biomaterials*. 2013; 34:8042–8048. [PubMed: 23896005]
37. Nemir S, Hayenga HN, West JL. PEGDA hydrogels with patterned elasticity: novel tools for the study of cell response to substrate rigidity. *Biotechnology and bioengineering*. 2010; 105:636–644. [PubMed: 19816965]
38. Dugas V, Chevalier Y. Surface hydroxylation and silane grafting on fumed and thermal silica. *Journal of colloid and interface science*. 2003; 264:354–361. [PubMed: 16256651]
39. Yoshida W, Castro RP, Jou J-D, Cohen Y. Multilayer alkoxy silane silylation of oxide surfaces. *Langmuir : the ACS journal of surfaces and colloids*. 2001; 17:5882–5888.
40. Muir BV, Myung D, Knoll W, Frank CW. Grafting of cross-linked hydrogel networks to titanium surfaces. *ACS Appl Mater Interfaces*. 2014; 6:958–966. doi:10.1021/am404361v. [PubMed: 24364560]
41. Cha C, et al. Tailoring hydrogel adhesion to polydimethylsiloxane substrates using polysaccharide glue. *Angewandte Chemie International Edition*. 2013; 52:6949–6952.
42. Stile RA, Barber TA, Castner DG, Healy KE. Sequential robust design methodology and X - ray photoelectron spectroscopy to analyze the grafting of hyaluronic acid to glass substrates. *Journal of biomedical materials research*. 2002; 61:391–398. [PubMed: 12115464]

43. Bai Y, et al. Transparent hydrogel with enhanced water retention capacity by introducing highly hydratable salt. *Applied Physics Letters*. 2014; 105:151903.
44. Yang CH, et al. Ionic cable. *Extreme Mechanics Letters*. 2015

Author Manuscript

Author Manuscript

Author Manuscript

Author Manuscript

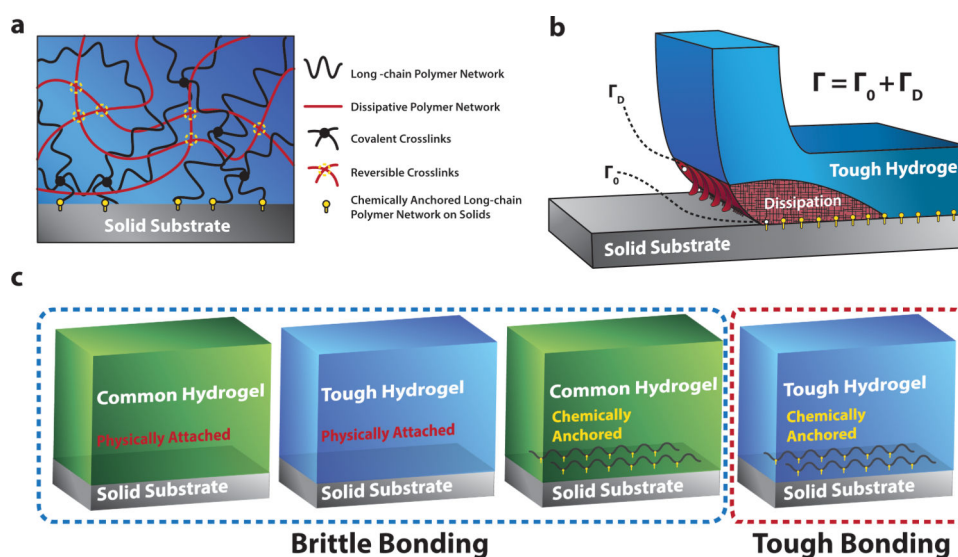


Figure 1. A design strategy for tough bonding of hydrogels to diverse solids

a. The tough bonding first requires high fracture toughness of constituent hydrogels. Whereas tough hydrogels generally consist of long-chain polymer networks and mechanically dissipative components, it is sufficient to achieve tough bonding by chemically anchoring the long-chain networks on solid surfaces. **b.** The chemical anchoring gives a relatively high intrinsic work of adhesion Γ_0 , which maintains cohesion of the hydrogel-solid interface and allows large deformation and mechanical dissipation to be developed in the hydrogel during detachment. The dissipation further contributes to the total interfacial toughness by Γ_D . **c.** Schematics of various types of hydrogel-solid interfaces to be tested in the current study to validate the proposed design strategy (from left to right): common and tough hydrogels physically attached on solids, and common and tough hydrogels chemically anchored on solids.

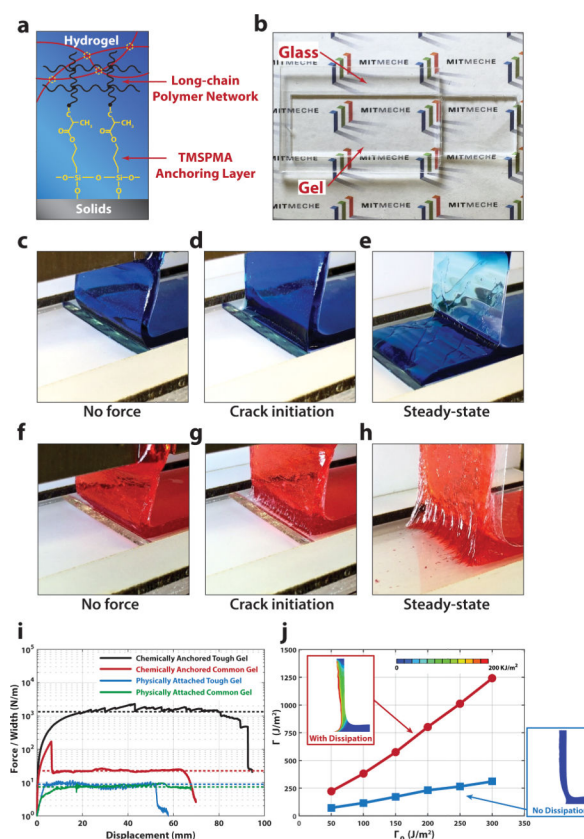


Figure 2. Experimental and modeling results on various types of hydrogel-solid bonding
a. The chemical anchoring of long-chain polymer networks is achieved by crosslinking the networks to functional silanes grafted on the surfaces of various solids. **b.** The high transparency of the hydrogel-solid bonding is demonstrated by a colorful logo “MIT MECH” behind a hydrogel-glass hybrid. **c-e.** Photos of the peeling process of a common hydrogel chemically anchored on a glass substrate. **f-h.** Photos of the peeling process of a tough hydrogel with its long-chain network chemically anchored on a glass substrate. (Note that blue and red food dyes are added into the common and tough hydrogels, respectively, to enhance the contrast of the interfaces.) **i.** The curves of peeling force per width of hydrogel sheet vs. displacement for various types of hydrogel-solid bonding. **j.** The calculated interfacial fracture toughness Γ as a function of the prescribed intrinsic work of adhesion Γ_0 in finite-element models for the tough hydrogel and a pure elastic hydrogel with no mechanical dissipation but otherwise the same properties as the tough hydrogel. The contours in the inset figures indicate mechanical energy dissipated per unit area.

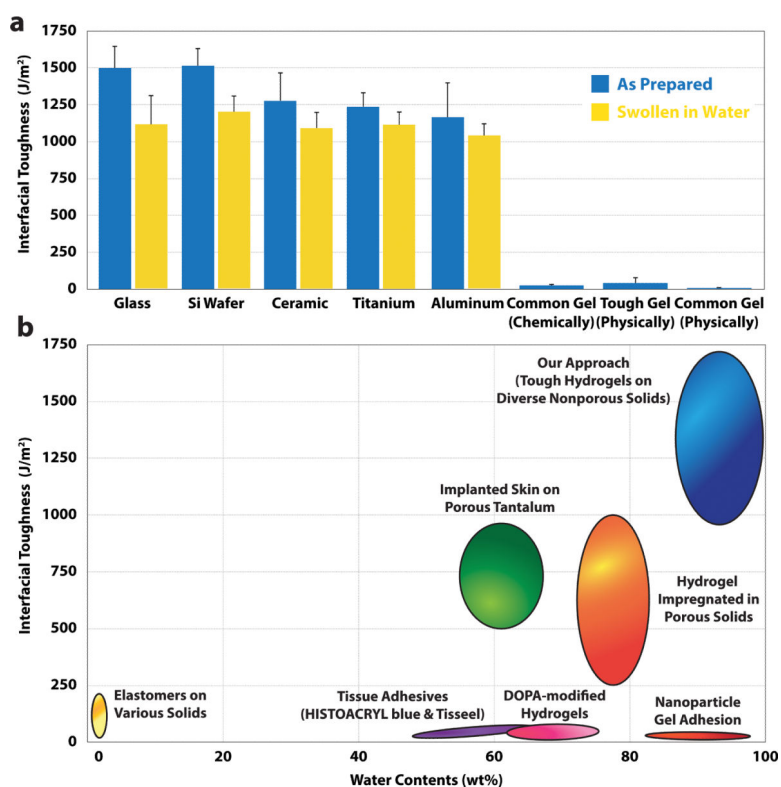


Figure 3. Performance of the tough bonding of hydrogels to various solids

a. Measured interfacial toughness of PAAm-alginate hydrogel bonded on glass, silicon wafer, ceramic, titanium and aluminum are consistently high, over 1000 Jm^{-2} , at both as-prepared and swollen states. In contrast, the interfacial toughness of the control samples are very low, $8 - 20 \text{ Jm}^{-2}$, at as prepared state. (Since the control samples debond from solids at fully swollen state, the interfacial toughness is not measured.) **b.** Comparison of interfacial toughness of PAAm-alginate hydrogel bonded on diverse solids and other hydrogel-solid bonding commonly used in engineering applications as functions of water concentrations in the hydrogels. DOPA in **b** represents 3,4-dihydroxyphenyl-L-alanine. Values in **a.** represent mean and standard deviation ($n = 3-5$).

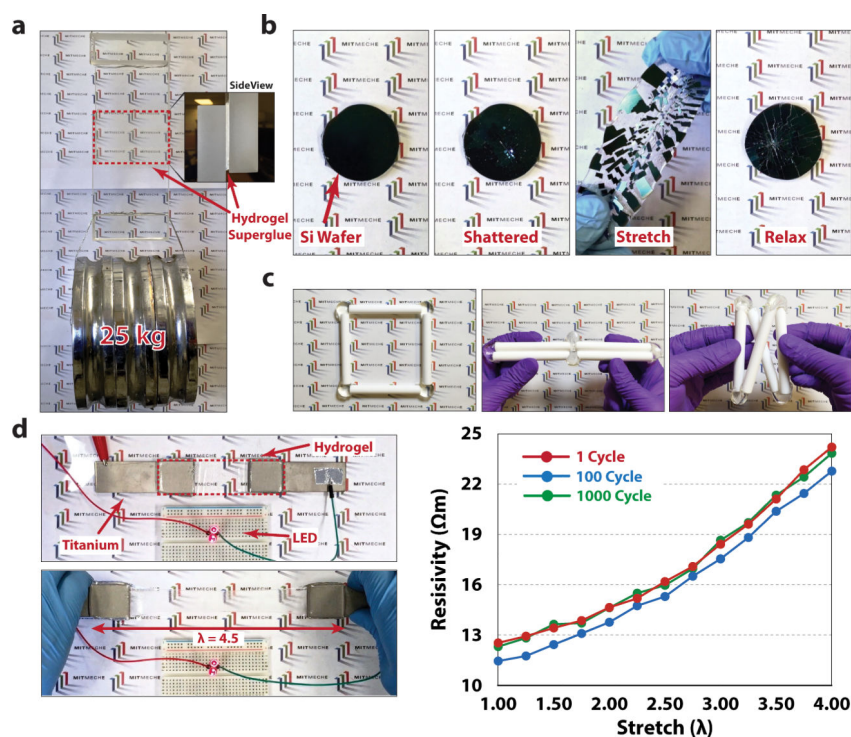


Figure 4. Novel applications of hydrogel-solid hybrids enabled by the tough bonding
a. Two glass plates bonded by the hydrogel superglue (dimension, 5 cm \times 5 cm \times 1.5 mm) are transparent, and can readily sustain a weight of 25 kg. **b.** The tough bonding of hydrogel to a silicon wafer gives a new coating that is mechanically protective. Shattered silicon chips still tightly attach on the hydrogel coating even under high stretches. **c.** The tough hydrogel bonding act as flexible but robust joints between four ceramic bars, which can be deformed into different configurations. **d.** The tough bonding of an ion-containing hydrogel on two titanium electrodes is conductive enough to power a LED light, even when the hydrogel is under high stretch of 4.5 times. The conductivity of the hydrogel-metal hybrid maintains almost the same even after 1000 cycles of high stretch up to 4 times.